Mll-COMPASS complexes mediate H3K4me3 enrichment and transcription of the osteoblast master gene Runx2/p57 in osteoblasts

Adriana Rojas[1,2,3,*], **Hugo Sepulveda**[2,3], **Berta Henriquez**[4], **Rodrigo Aguilar**[2,3], **Tatiana Opazo**[2,3], **Gino Nardocci**[2,3], **Fernando Bustos**[2,3], **Jane B. Lian**[5], **Janet L. Stein**[5], **Gary S. Stein**[5], **Brigitte van Zundert**[2], **Andre J. van Wijnen**[6], **Miguel L. Allende**[3,7], **Martin Montecino**[2,3,*]

[1]Institute of Human Genetics, Faculty of Medicine, Pontificia Universidad Javeriana, Bogota, Colombia

[2]Institute of Biomedical Sciences, Faculty of Medicine and Faculty of Life Sciences, Universidad Andres Bello

[3]FONDAP Center for Genome Regulation, Santiago, Chile

[4]Faculty of Science, Universidad San Sebastián, Santiago, Chile

[5]Department of Biochemistry, University of Vermont College of Medicine, Burlington, VM, USA

[6]Mayo Clinic, Rochester, MN, USA

[7]Department of Biology, Faculty of Sciences, Universidad de Chile, Santiago, Chile

Abstract

Expression of Runx2/p57 is a hallmark of the osteoblast-lineage identity. While several regulators that control the expression of Runx2/p57 during osteoblast lineage commitment have been identified, the epigenetic mechanisms that sustain this expression in differentiated osteoblasts remain to be completely determined. Here we assess epigenetic mechanisms associated with Runx2/p57 gene transcription in differentiating MC3T3 mouse osteoblasts. Our results show that an enrichment of activating histone marks at the Runx2/p57 P1 promoter is accompanied by the simultaneous interaction of Wdr5 and Utx proteins, both components of COMPASS complexes. Knockdown of Wdr5 and Utx expression confirms the activating role of both proteins at the Runx2 P1 promoter. Other chromatin modifiers that were previously described to regulate Runx2/p57 transcription in mesenchymal precursor cells (Ezh2, Prmt5 and Jarid1b proteins) were not found to contribute to Runx2/p57 transcription in full-committed osteoblasts. We also determined the presence of additional components of COMPASS complexes at the Runx2/p57 promoter, evidencing that the Mll2/COMPASS- and Mll3/COMPASS-like complexes bind to the P1 promoter in osteoblastic cells expressing Runx2/p57 to modulate the H3K4me1 to H3K4me3 transition.

*To whom correspondence can be addressed: Instituto de Ciencias Biomedicas, Facultad de Medicina, Universidad Andres Bello, Avenida Republica 239, Santiago, Chile. mmontecino@unab.cl; Instituto de Genetica Humana, Facultad de Medicina, Pontificia Universidad Javeriana, Bogota, Colombia. rojas-adriana@javeriana.edu.co.

Keywords

Runx2; osteoblast differentiation; epigenetic control of osteoblast gene transcription

Introduction

During mammalian development, the mesenchymal-osteoblast transition requires the function of master transcriptional regulators, including Runx2 (Karsenty, 2008; Komori, 2018; Marie, 2008; Meyer et al., 2014; Wu et al., 2014). This factor has been shown to play a principal role in the process as it controls the expression of a significant number of down-stream bone-related target genes (Stein et al., 2004). We and others, have shown that transcription of Runx2/p57, the bone-specific isoform of this factor, is mainly controlled by the P1 promoter sequence, in particular, through the first 500 bp upstream of the transcriptional start site (TSS) (Drissi et al., 2000; Hovhannisyan et al., 2013; Tai et al., 2014; Xiao et al., 2001). Importantly, this region exhibits chromatin remodeling in cells expressing the gene, as reflected by increased DNase I hypersensitivity, through a process that occurs independently of SWI/SNF chromatin remodeling activity (Brg1- and Brm-containing complexes) (Cruzat et al., 2009).

It has been recently demonstrated that the expression of Runx2/p57 is epigenetically controlled through chromatin complexes that catalyze post-translational modifications at the histones associated with the Runx2 P1 promoter (Aguilar et al., 2016; Rojas et al., 2015; Sepulveda et al., 2017a; Tai et al., 2014; Yang et al., 2013; Zhang et al., 2015). Hence, silencing of this gene in non-osseous cells is tightly associated with the activity of the Polycomb PRC2 repressive complex that mediates the deposition of the histone H3 lysine 27 trimethylation (H3K27me3) mark (Aguilar et al., 2016; Rojas et al., 2015). Also, it was shown that complexes containing the subunits Wdr5 and Utx/Kdm6a can mediate deposition and elimination of epigenetic histone marks (H3K4me3 and H3K27me3, respectively) that accompany transcriptional activation of the Runx2/p57 gene during commitment of mesenchymal cells to the osteoblast lineage (Rojas et al., 2015). Interestingly, previous reports also indicate that increased expression of Wdr5 promotes the osteoblast gene expression program both in vivo and in vitro (Aguilar et al., 2016; Gori and Demay, 2004; Gori et al., 2001; Gori et al., 2006; Zhu et al., 2008). Wdr5 binds to the Runx2-P1 proximal promoter region and mediates Runx2/p57 transcriptional up-regulation (Aguilar et al., 2016; Gori et al., 2006; Rojas et al., 2015). Hence, there is a direct link between the function of Wdr5-containing complexes and the mechanisms that control Runx2 transcription.

Similarly, other epigenetic "writers" and "erasers", including arginine methylase Prmt5 and lysine demethylase Jarid1b/Kdm4b have been shown to mediate deposition and elimination of epigenetic histone marks at the P1 promoter (H4R3me2s and H3K4me3, respectively) that accompany transcriptional activation and repression of the Runx2/p57 gene during commitment of mesenchymal cells to the osteoblastic, myoblastic or adipogenic lineages (Bustos et al., 2017; Rojas et al., 2015). Moreover, it was found that maintaining increased levels of the marks H3K27ac and H3K4me3 at the P1 promoter (by knocking down Jarid1b expression) prevents Runx2/p57 gene silencing in mesenchymal cells induced to

differentiate to myoblasts (Rojas et al., 2015). Nevertheless, the contribution of these key epigenetic regulators during differentiation of already committed pre-osteoblastic cells has not been defined.

Here we take advantage of the ability of pre-osteoblastic MC3T3 cells to differentiate in culture to osteoblasts, expressing early and late bone phenotypic markers (Wang et al., 1999), to determine the role of specific epigenetic mechanisms during this process. We report that Trithorax/COMPASS-like complexes, including the Wdr5 and Utx subunits, are increasingly enriched at the Runx2-P1 promoter sequence during osteoblast differentiation. The P1 promoter-bound complexes also include the Mll2 and Mll3 histone H3K4 methylases and can then mediate the elevated H3K4me3 levels found at this promoter in cells actively transcribing Runx2/p57.

Experimental procedures

Mouse pre-osteoblastic MC3T3 cells (donated by Dr. Rafael Burgos, Universidad Austral de Chile, Valdivia, Chile) were maintained in α-MEM without ascorbic acid (AA) (catalog number A10490–01, Thermo Fisher, Waltham MA, USA) and supplemented with 10% FBS and 2.29 g/liter $NaHCO_3$ (Wang et al., 1999). When required, MC3T3 cells were grown to confluence and induced to differentiate into osteoblasts by supplementing the medium with A (50 μg/ml) from day 3 of culture. Rat osteosarcoma-derived ROS 17/2.8 cells (Majeska et al., 1980) were maintained in F-12 medium (catalog number 21700–075, Thermo Fisher) supplemented with 5% FBS, 1.176 g/liter $NaHCO_3$, 0.118 g/liter $CaCl_2x2H_2O$, and 6.670 g/liter HEPES (Life Technologies). Rat hepatoma H-4-II-E cells were maintained in α-MEM medium (catalog number 11900–024, Thermo Fisher) supplemented with 2,29 g/liter $NaHCO_3$ and 10% FBS. Mouse N2a neuroblastoma cells were maintained in D-MEM medium (catalog number 11965–092, Thermo Fisher) supplemented 10% FBS and induced to differentiation by serum deprivation following described protocols (Hou et al., 2008; Ma et al., 2015; Sontag et al., 2010). To detect alkaline phosphatase activity, the cells were washed with ice-cold phosphate buffered saline (PBS), fixed with paraformaldehyde 37%:ethanol 1:1, and stained with NBT/BCIP (Roche, Basel, Switzerland) for 30 min at 37°C.

Lentivirus production and infection of MC3T3 cells.

HEK293FT cells (Life Technologies) were grown in 60 mm culture plates to 80–90% confluence. Lipofectamine 2000 reagent (Life Technologies) was used to transfect cells (following the manufacturer's instructions) with the pCMV-VSVg, pCMV-dR8.91 and pLKO.1-shRNA plasmids (at a 1:2:3 ratio, respectively; plasmids donated by Dr. Pedro Zamorano, Universidad de Antofagasta, Chile) with a maximum total DNA amount of 10 μg per plate. pLKO.1 EV (empty vector) was used as a control. After 16–18 h, the culture medium was replaced and cells were maintained at 32 °C for 48 h. Supernatants containing pseudo-typed particles were collected, filtered through a PVDF filter (0.45 μm pore size). Aliquots of supernatants were immediately stored at −80 °C. MC3T3 cells were plated in 6-well culture plates and infected for 48 h with 300 μl lentiviral particles containing shRNA-Wdr5, shRNA-Jarid1b, shRNA-Ezh2, shRNA-Utx, shRNA-Prmt5 or EV plasmids. All short

hairpin-containing plasmids were acquired at Open Biosystems (GE Healthcare Dharmacon, Lafayette, CO, USA).

Nuclear extracts and protein expression analyses.

Nuclear extracts were prepared as reported previously (Paredes et al., 2004). The protein levels were quantified by Bradford's assay using bovine serum albumin as a standard. For western blot analyses, 10 μg of total protein was subjected to SDS-polyacrylamide gel electrophoresis (PAGE) and then transferred to nitrocellulose membrane. Immunoblotting was performed with secondary antibodies conjugated to horseradish peroxide and enhanced chemiluminescence solutions (Perkin-Elmer, Boston, MA, USA). Primary antibodies used were the following: Gapdh (ab9485, Abcam, Cambridge, MA, USA), αTFIIB C-18 (sc-225, Santa Cruz Biotechnology, Dallas, TX, USA), RNA-PolII N-20 (sc-899, Santa Cruz Biotechnology), Runx2 S-19 (sc-12488, Santa Cruz Biotechnology), Wdr5 (ab56919, Abcam), JARID1B/KDM4B (ab50958, Abcam), Ezh2 (39901, Active Motif, Carlsbad, CA, USA), Utx/Kdm6A (ab91231, Abcam), Prmt5/Jbp1 (611539, BD Biosciences, San Jose, CA, USA).

Reverse transcriptase and quantitative real-time PCR (RT-qPCR).

Total RNA was extracted with TRIzol (Life Technologies), according to the manufacturer's protocol. An equal amount of each sample (2 μg) was used for reverse transcription. qPCR was performed using Brilliant II SYBR® Green QPCR Master Mix (Agilent Technologies, Santa Clara, CA, USA). Data are presented as relative mRNA levels of the gene of interest normalized to Gapdh mRNA levels. Primer used were: Runx2/p57 Fw: TCT GGA AAA AAGG AGG GAC TAT G, Rev: GGT GCT CGG ATC CCA AAA GAA, mouse Bglap Fw: CTG AGT CTG ACA AAG CCT TC, Rev: CTG GTC TGA TAG CTC GTC AC, rat Bglap Fw: CTG AGT CTG ACA AAG CCT TC, Rev: GTG GTC CGC TAG CTC GTC AC, Wdr5 Fw: CCA GTC CAA CCT CAT CGT CT, Rev: CAT CAC GGT TGA AAT GAA CG; Jarid1b Fw: AGT GGC TTT CCT GTT CGA GA, Rev: AAG CAC ATG CCC ACA TAC AA; Ezh2 Fw: CAT TTC ATA CGC TCT TCT GTC GAC, Rev: CCC TCC AGA TGC TGG TAA CAC T; Utx Fw: ACA GTA ATA CGT GGC CTT GCT GGA, Rev: TTC ATC TGC TGG TTG TAA CAA CTG; Prmt5 Fw: GGA ACT CTG AAG CGG CTA TG, Rev: GTG TGT AGT CGG GGC ATT CT; Gapdh Fw: CAT GGC CTT CCG TGT TCC TA, Rev: CCT GCT TCA CCA CCT TCT TGA T.

Chromatin immunoprecipitation.

Chromatin immunoprecipitation (ChIP) assays were performed in cross-linked chromatin samples as described earlier (Soutoglou and Talianidis, 2002), with the following modifications. Cells were washed with cold PBS 1X buffer, incubated for 10 min with 1% formaldehyde (FA) at room temperature and washed again with PBS 1X. For ChIP against chromatin-modifying enzymes, we used double cross-linking with EGS (Ethylene glycol-bis(succinicacid N-hydroxysuccinimide ester; E3257, Sigma, St. Louis, MO, USA) (Zeng et al., 2006): the FA cross-linked cells were incubated with EGS for 1 h at room temperature with gentle agitation, washed three times with cold PBS, resuspended in 1 ml of cell lysis buffer (CLB; 5 mM Hepes, pH 8.0, 85 mM KCl, Triton X-100 and proteinase inhibitors), and homogenized with a Dounce homogenizer (~25 times using a tight pestle). The cell

extract was collected by centrifugation at 3000 ×g for 5 min, resuspended in 0.5ml of sonication buffer (50 mM Hepes, pH 7.9, 140 mM NaCl, 1 mM EDTA, 1% Triton X-100, 0.1% deoxycholate acid, 0.1% SDS, and a mixture of proteinase inhibitors), and incubated for 10 min on ice. Chromatin extracts were sonicated at high power for six pulses of 5 min each, 30 sec on, 30 sec off in a water bath sonicator Bioruptor (Diagenode, Liege, Belgium) and centrifuged at $16,000 \times g$ for 15 min at 4 °C to obtain fragments of 500 bp or smaller. The supernatant was collected, aliquoted, frozen in liquid nitrogen, and stored at −80 °C; one aliquot was used for A260 measurements. Chromatin size was confirmed by electrophoretic analysis. Cross-linked chromatin extracts (2 A_{260} units) were re-suspended in sonication buffer to a final volume of 500 μl; samples were pre-cleared by incubating with 2–4 μg of normal IgG and 50 μl of protein A/G-agarose beads (Santa Cruz Biotechnology) for 1 h at 4 °C with agitation. Chromatin was centrifuged at 4000 ×g for 5 min, the supernatant was collected, and was immunoprecipitated with specific antibodies (see list below for antibodies used) for 12–16 h at 4 °C. The immune complexes were recovered with addition of 50 μl of protein A or G-agarose beads, followed by incubation for 1 h at 4 °C with gentle agitation. Immunoprecipitated complexes were washed once with sonication buffer, twice with LiCl buffer (100 mM Tris–HCl, pH 8.0, 500 Mm LiCl, 0.1% Nonidet P40, and 0.1% deoxycholic acid), and once with Tris–EDTA (TE) buffer pH 8.0 (2 mM EDTA and 50 mM Tris–HCl, pH 8.0), each time for 5 min at 4 °C; this was followed by centrifugation at 4000 ×g for 5 min. The protein–DNA complexes were eluted by incubation with 100 μl of elution buffer (50 mM NaHCO3 and 1% SDS) for 15 min at 65 °C. Extracts were centrifuged at 10,000 ×g for 5 min, and the supernatant was collected and incubated for 12–16 h at 65 °C, to reverse the cross-linking. Proteins were digested with 100 μg/ml of proteinase K for 2 h at 50 °C, and the DNA was recovered by phenol/chloroform extraction and ethanol precipitation using glycogen (20 μg/ml) as a precipitation carrier. The qPCR primers used to evaluate the Runx2-P1 promoter region were: forward, 5′-GTG GTA GGC AGT CCC ACT TT-3′; reverse, 5′-TGT TTG TGA GGC GAA TGA AG-3′. For the −5Kb sequence located upstream of the Ric8b gene promoter (control region): forward, 5'-CATGGACAGGGTTTTGGGAGAC-3'; reverse, 5'-ACCTGTAGGTTCTGTGCATCTC-3'.

The following antibodies were used in ChIP assays: Wdr5 (ab56919, Abcam), Jarid1b/Kdm4b (ab50958, Abcam), Ezh2 (07–689, Merck Millipore, Danvers, MA, USA), Utx/Kdm6a (ab91231, Abcam), Prmt5/Jbp1 (611539, BD Biosciences), H3K27me3 (07–449, Merck Millipore), H3K4me1 (ab8895, Abcam), H3K4me3 (ab8580, Abcam), H4R3me2S (ab5823, Abcam), H3Ac (06–599, Merck Millipore), Cgbp (SC-25391, Santa Cruz Biotechnology), Menin (A300–105A, Bethyl Laboratories, Montgomery, TX, USA), Set1A (A300–290A, Bethyl Laboratories), Set1B (SC-248563, Santa Cruz Biotechnology), Mll1 (39829, Active Motif), Mll2 (SC-292359, Santa Cruz Biotechnology), Mll3 (ab71200, Abcam), Mll4 (ab60053, Abcam). Re-ChIP assays were performed as described (Cruzat et al., 2009). Briefly, the immunoprecipitated complexes obtained by ChIP were eluted by incubation for 30 min at 37 °C in 25 μl of 10mM dithiothreitol. After centrifugation, the supernatant was diluted 20 times with sonication buffer and subjected to the ChIP procedure with the second antibody.

Statistical analyses

For ChIP assays, we used a one-way ANOVA analysis followed by the Dunnett post-test to compare significant changes with respect to control. For mRNA expression analysis, we used the Student's t-test. In all figures, error bars represent the mean $\pm$ SEM; *P < 0.05, **P < 0.01, ***P < 0.001.

RESULTS

Runx2/p57 expression during progression of osteoblast differentiation is epigenetically controlled

Chromatin immunoprecipitation (ChIP) analyses indicate that the proximal Runx2 P1 promoter region exhibits post-translational modifications at histones H3 and H4 (H3 and H4 marks) that are characteristic of transcriptionally active genes in osteoblastic ROS17/2.8 cells (OB), constitutively expressing Runx2/p57, versus hepatoma H4-II-E cells (He) that do not (Fig. 1A). These modifications include elevated histone H3 acetylation (H3Ac; Fig. 1B) and tri-methylation of K4 (H3K4me3; Fig. 1C), as well as reduced H3K4me1 (Fig. 1D) and H3K27me3 (Fig. 1E). In addition, transcription of the Runx2/p57 gene is accompanied by reduced symmetric di-methylation at the arginine 3 residue of histone H4 (H4R3me2s, Fig. 1F), a mark that has been reported to be principally enriched in regulatory regions of transcriptionally repressed genes (Fabbrizio et al., 2002), although this role has been recently challenged (Rojas et al., 2015). These data collectively indicate that the transcriptionally active state of the P1 promoter in osteoblastic cells involves a profile characterized by enrichment of H3Ac and H3K4me3, as well as reduced levels of H3K4me1, H3K27me3, and H4R3me2s.

MC3T3 cells are pre-osteoblastic mesenchymal cells that progressively differentiate to mineralized osteoblasts when grown in the presence of ascorbic acid (AA), thus representing a well-established model system to study gene regulation during osteogenesis (Wang et al., 1999). Differentiating MC3T3 cells exhibit increased mRNA expression of genes associated with the osteoblast lineage, including Runx2/p57 and Bglap (Fig. 2A), and elevated alkaline phosphatase (AP) activity associated with the extracellular matrix of these cells (Fig. 2B). Importantly, the increase in Runx2/p57 expression during MC3T3 osteoblast differentiation is paralleled by enrichment of H3Ac (Fig. 2C), H3K4me3 (Fig. 2D) and H3K27Ac (Fig. 2E) marks at the proximal P1 promoter region. Reduced levels of H3K27me3 (Fig. 2F) and H4R3me2s marks (Fig. 2G) were detected in the P1 promoter sequence at all stages of differentiation that were analyzed. The latter result is in agreement with the proposed model indicating that these repressive epigenetic marks are diminished during early-stages of osteogenic cell fate determination that are prior to full commitment to the osteoblast lineage (Rojas et al., 2015).

Runx2 P1 proximal promoter is enriched in epigenetic regulators that mediate histone modifications associated with Runx2/p57 transcription

To determine regulatory components mediating the epigenetic changes associated with transcriptional control of the Runx2/p57 gene during osteoblast differentiation, we carried out ChIP analyses against known epigenetic regulators that can mediate these marks. We

first used specific antibodies against these proteins to confirm by western blot their presence in nuclear extract samples obtained from MC3T3 cells at different stages of differentiation (Fig. 3A). Among the proteins analyzed, we detected that Wdr5 and Utx, two main components of Mll/COMPASS-like complexes including H3K4 methyltransferase (H3K4me3) and H3K27 demethylase (H3K27me3) activities (Shilatifard, 2012), are expressed during MC3T3 osteoblast differentiation. Similarly, Ezh2 (the catalytic subunit of PcG that mediates H3K27me3), Jarid1b (H3K4me3 demethylase) and Prmt5 (H4R3me2s methyltransferase) are expressed in differentiating MC3T3 osteoblastic cells.

ChIP analyses show, however, that only Wdr5 and Utx are bound to the Runx2 P1 proximal promoter in MC3T3 cells expressing Runx2/p57 (Fig. 3B and 3C, respectively). Moreover, binding of Wdr5 and Utx is significantly increased upon osteoblast differentiation (Fig. 3B and 3C, compare DIV 3 and DIV 8). Importantly, both proteins bind simultaneously to the P1 promoter as this proximal genomic sequence is detected in a re-ChIP experiment where chromatin is first precipitated with the anti-Utx antibody and subsequently re-precipitated with the anti Wdr5 antibody (Fig. 3D). These results suggest that a Mll/COMPASS-like complex containing these two subunits can bind and mediate the enrichment of H3K4me3 and the reduction of H3K27me3 at the Runx2 P1 promoter that accompanies transcription of the Runx2/p57 isoform. Other relevant epigenetic regulators, including Ezh2, Prmt5, and Jarid1b are not found significantly associated with the Runx2 P1 promoter region in differentiating MC3T3 osteoblastic cells (Figs 3E, 3F, and 3G, respectively).

Wdr5 and Utx are required for transcription of Runx2/p57 in differentiating osteoblasts

To directly assess whether transcription of Runx2/p57 during MC3T3 osteoblast differentiation is epigenetically-controlled by chromatin-associated complexes that contain Wdr5 and Utx, we carried out knockdown experiments using specific lentiviral-driven shRNAs that target the mRNAs encoding these proteins. shRNA-mediated Wdr5-knockdown (Fig. 4A, left), results in a significant inhibition of Runx2/p57 mRNA expression (Fig. 4A, right). Similarly, Utx-knockdown in these cells (Fig. 4B, left) significantly inhibits Runx2/p57 mRNA increase (Fig. 4B, right). Together, these results further demonstrate that binding of a complex containing Wdr5 and Utx (Mll/COMPASS-like complex) to the P1 promoter enhances Runx2/p57 expression in osteoblasts. Impaired osteoblast differentiation due to reduced Runx2/p57 expression following Wdr5- and Utx-knockdown was confirmed by decreased Bglap mRNA expression, a well-established osteoblast-late phenotypic gene marker that is directly up-regulated by Runx2 (Banerjee et al., 1996; Ducy et al., 1997) (Fig. 4C).

In contrast, knockdown of either Ezh2 (Fig. 4D) or Prmt5 (Fig. 4E) expression in differentiating MC3T3 cells does not significantly affect mRNA expression of either Runx2/p57 (Fig. 4C and 4D) or Bglap (not shown) genes. This result is in accordance with the reduced interaction of these H3K27 and H4R3 methyltransferases, respectively, with the Runx2 P1 promoter region in these osteoblastic cells (see Fig. 3).

We have recently shown that during mesenchymal-myogenic lineage commitment H3K4me3 demethylase Jarid1b plays a major role by reducing this epigenetic mark at the Runx2 P1 promoter and hence inhibiting Runx2/p57 transcription (Rojas et al., 2015). It was

important then to evaluate in MC3T3 differentiating osteoblasts the contribution of Jarid1b to Runx2/p57 expression. As shown in Fig. 5 knockdown of Jarid1b in these cells only marginally increases Runx2/p57 mRNA expression. This result is in agreement with the low enrichment of this H3K4me3 demethylase at the Runx2 P1 promoter in these cells (see Fig. 3G). Also, this result indicates that this enzyme has a minor role in modulating Runx2/p57 transcription in cells already committed to the osteoblastic lineage.

Because our results indicated that a Mll-COMPASS-like complex is playing a relevant role during transcription of the Runx2/p57 gene in differentiating osteoblastic cells, it was next determined whether additional subunits (besides Wdr5 and Utx) of these H3K4 methyltransferase complexes were bound to the Runx2 P1 promoter (Fig. 6). It was found that neither Set1a/Set1b nor Cgbp, all critical components of Set-COMPASS complexes, were highly enriched at the P1 promoter (Fig. 6A). In contrast, Mll2 (but not Mll1) and Menin, both components of the Mll2-COMPASS-like complexes are enriched at this Runx2 P1 promoter sequence (Fig. 6A). Similarly, Mll3 (but not Mll4) is found binding to this promoter in Runx2/p57 expressing MC3T3 osteoblasts, indicating that a Mll3-COMPASS-like complex interacts with this regulatory region. To control for cell specificity of these protein-chromatin interactions, we determined that none of these epigenetic regulators bind to this promoter region in mouse neuronal cells (Fig. 6B), where the Runx2/p57 gene is not expressed (Aguilar et al., 2016).

Together these results indicate that both Mll2- and Mll3-COMPASS complexes bind to the Runx2 P1 promoter and are, therefore, capable of establishing the H3K4me3 state that promotes and sustains the expression of this bone-master gene in osteoblasts.

DISCUSSION

Expression of Runx2/p57 is critical for establishing the osteoblast phenotype, a process that is tightly controlled through epigenetic mechanisms (Aguilar et al., 2016; Meyer et al., 2014; Rojas et al., 2015; Tai et al., 2014; Wu et al., 2014). Among these mechanisms, a specific profile of histone modifications at the Runx2 P1 promoter has been shown to play a pivotal role in determining the lineage-specific expression of this bone-master regulator (Bustos et al., 2017; Rojas et al., 2015; Sepulveda et al., 2017a; Tai et al., 2014). Here ChIP analyses confirm an epigenetic profile at the proximal P1 promoter region that is mainly characterized by enrichment of H3Ac and H3K4me3 and reduced levels of H3K4me1, H3K27me3 and H4R3me2s. Our complementary analyses indicate that enhanced Runx2/p57 expression in osteoblasts is not sustained merely by the absence of repressive mechanisms, but that also requires the contribution of activator complexes. Importantly, the presence of H3Ac and H4K3me3 further evidences the regulatory role of histone acetyl-transferases (HATs) and H3K4 methylases during activation of Runx2/p57 gene transcription.

Recent reports from our team and others have demonstrated a role of p300 in both depositing and maintaining histone acetylation at the Runx2 P1 promoter (Rojas et al., 2015; Wu et al., 2014) as well as at other relevant genes for the osteoblastic phenotype (Sepulveda et al., 2017b). These and other reports have also indicated a role for Mll-COMPASS complexes in mediating H3K4me3 enrichment at the Runx2 P1 promoter and transcriptional

activity of this gene (Aguilar et al., 2016; Rojas et al., 2015; Yang et al., 2017). Thus, a recent publication demonstrates the contribution of Phf20 (H3K4me reader protein) to Runx2 transcription during osteoblast differentiation (Yang et al., 2017). The authors suggest that this Phf20-dependent increase in Runx2/p57 transcription and H3K4me3 enrichment at the P1 promoter region is due to its ability to interact with Mll-containing complexes and to stimulate their H3K4 methylating activity (Yang et al., 2017). Our re-ChIP analysis confirms the interaction of a Wdr5/Utx-containing complex with the Runx2/p57 promoter. Moreover, the experiments that silence the expression of Wdr5 and Utx strongly support the functional role of both proteins on the Runx2/p57 transcription process.

Our group previously described the binding of the H3K4me3 demethylase Jarid1b to the Runx2 P1 promoter and the pivotal role of this enzyme during Runx2/p57 gene repression in uncommitted mesenchymal cells (Bustos et al., 2017; Rojas et al., 2015). ChIP analyses here, however, indicate that this is not the case in MC3T3 pre-osteoblasts. Moreover, the absence of Jarid1b at the Runx2 P1 promoter occurs albeit the Jarid1b protein is highly expressed in these osteoblastic cells. This absence of Jarid1b enrichment suggests then that the minor increase in Runx2/p57 mRNA expression detected in cells were Jarid1b was knockdown is indirect.

It has been largely known that gene transcription efficacy is the final resultant of the balance in the function of repressor and activator complexes. H3K4me3 levels at the Runx2 P1 promoter region can be defined by histone methyltransferase- and histone demethylase-containing complexes that enhance and reduce this epigenetic mark, respectively. Therefore, our data support a model where H3K4me3 enrichment at the Runx2 P1 promoter in osteoblasts is selectively maintained by the recruitment of COMPASS-like complexes together with a reduced interaction of Jarid1b. The specific mechanisms involved in this selective release of Jarid1b from the P1 promoter during osteoblast differentiation are currently under investigation.

It remains to be established whether Mll2- and Mll3-containing complexes mediate redundant, complementary or perhaps opposite functions at the transcriptionally active Runx2 P1 promoter. Recent reports indicate that interaction of two or more different COMPASS and COMPASS-like complexes at particular regulatory regions can contribute to up- or down-regulate transcription, as it may result in enrichment of the H3K4me3 or H3K4me1 marks, respectively (Cheng et al., 2014; Hu et al., 2013; Nayak et al., 2014; Wang et al., 2009). Therefore our work provides new evidence showing that an epigenetic mechanism involving the transition from H3K4me1 to H3K4me3 can represent a critical step during transcriptional activation of the Runx2 master regulator of osteogenesis.

ACKNOWLEDGEMENTS

REFERENCES

Aguilar R, Bustos FJ, Saez M, Rojas A, Allende ML, van Wijnen AJ, van Zundert B, and Montecino M 2016 Polycomb PRC2 complex mediates epigenetic silencing of a critical osteogenic master regulator in the hippocampus. Biochimica et biophysica acta. 1859:1043–1055. [PubMed: 27216774]

Banerjee C, Hiebert SW, Stein JL, Lian JB, and Stein GS 1996 An AML-1 consensus sequence binds an osteoblast-specific complex and transcriptionally activates the osteocalcin gene. Proceedings of the National Academy of Sciences of the United States of America. 93:4968–4973. [PubMed: 8643513]

Bustos F, Sepulveda H, Prieto CP, Carrasco M, Diaz L, Palma J, Lattus J, Montecino M, and Palma V 2017 Runt-Related Transcription Factor 2 Induction During Differentiation of Wharton's Jelly Mesenchymal Stem Cells to Osteoblasts Is Regulated by Jumonji AT-Rich Interactive Domain 1B Histone Demethylase. Stem cells. 35:2430–2441. [PubMed: 28895234]

Cruzat F, Henriquez B, Villagra A, Hepp M, Lian JB, van Wijnen AJ, Stein JL, Imbalzano AN, Stein GS, and Montecino M 2009 SWI/SNF-independent nuclease hypersensitivity and an increased level of histone acetylation at the P1 promoter accompany active transcription of the bone master gene Runx2. Biochemistry. 48:7287–7295. [PubMed: 19545172]

Cheng J, Blum R, Bowman C, Hu D, Shilatifard A, Shen S, and Dynlacht BD 2014 A role for H3K4 monomethylation in gene repression and partitioning of chromatin readers. Molecular cell. 53:979–992. [PubMed: 24656132]

Drissi H, Luc Q, Shakoori R, Chuva S De Sousa Lopes JY Choi A Terry M Hu S Jones JC Neil JB Lian JL Stein AJ Van Wijnen, and Stein GS 2000 Transcriptional autoregulation of the bone related CBFA1/RUNX2 gene. Journal of cellular physiology. 184:341–350. [PubMed: 10911365]

Ducy P, Zhang R, Geoffroy V, Ridall AL, and Karsenty G 1997 Osf2/Cbfa1: a transcriptional activator of osteoblast differentiation. Cell. 89:747–754. [PubMed: 9182762]

Fabbrizio E, El Messaoudi S, Polanowska J, Paul C, Cook JR, Lee JH, Negre V, Rousset M, Pestka S, Le Cam A, and Sardet C 2002 Negative regulation of transcription by the type II arginine methyltransferase PRMT5. EMBO reports. 3:641–645. [PubMed: 12101096]

Gori F, and Demay MB 2004 BIG-3, a novel WD-40 repeat protein, is expressed in the developing growth plate and accelerates chondrocyte differentiation in vitro. Endocrinology. 145:1050–1054. [PubMed: 14657013]

Gori F, Divieti P, and Demay MB 2001 Cloning and characterization of a novel WD-40 repeat protein that dramatically accelerates osteoblastic differentiation. The Journal of biological chemistry. 276:46515–46522. [PubMed: 11551928]

Gori F, Friedman LG, and Demay MB 2006 Wdr5, a WD-40 protein, regulates osteoblast differentiation during embryonic bone development. Developmental biology. 295:498–506. [PubMed: 16730692]

Hou H, Obregon D, Lou D, Ehrhart J, Fernandez F, Silver A, and Tan J 2008 Modulation of neuronal differentiation by CD40 isoforms. Biochemical and biophysical research communications. 369:641–647. [PubMed: 18312851]

Hovhannisyan H, Zhang Y, Hassan MQ, Wu H, Glackin C, Lian JB, Stein JL, Montecino M, Stein GS, and van Wijnen AJ 2013 Genomic occupancy of HLH, AP1 and Runx2 motifs within a nuclease sensitive site of the Runx2 gene. Journal of cellular physiology. 228:313–321. [PubMed: 22886425]

Hu D, Garruss AS, Gao X, Morgan MA, Cook M, Smith ER, and Shilatifard A 2013 The Mll2 branch of the COMPASS family regulates bivalent promoters in mouse embryonic stem cells. Nature structural & molecular biology. 20:1093–1097.

Karsenty G 2008 Transcriptional control of skeletogenesis. Annual review of genomics and human genetics. 9:183–196.

Komori T 2018 Runx2, an inducer of osteoblast and chondrocyte differentiation. Histochemistry and cell biology.

Ma Q, Hu QS, Xu RJ, Zhen XC, and Wang GH 2015 Protease Omi facilitates neurite outgrowth in mouse neuroblastoma N2a cells by cleaving transcription factor E2F1. Acta pharmacologica Sinica. 36:966–975. [PubMed: 26238290]

Majeska RJ, Rodan SB, and Rodan GA 1980 Parathyroid hormone-responsive clonal cell lines from rat osteosarcoma. Endocrinology. 107:1494–1503. [PubMed: 6968673]

Marie P 2008 Transcription factors controlling osteoblastogenesis. Archives of biochemistry and biophysics. 473:98–105. [PubMed: 18331818]

Meyer MB, Benkusky NA, and Pike JW 2014 The RUNX2 cistrome in osteoblasts: characterization, down -regulation following differentiation, and relationship to gene expression. The Journal of biological chemistry. 289:16016–16031. [PubMed: 24764292]

Nayak A, Viale-Bouroncle S, Morsczeck C, and Muller S 2014 The SUMO-specific isopeptidase SENP3 regulates MLL1/MLL2 methyltransferase complexes and controls osteogenic differentiation. Molecular cell. 55:47–58. [PubMed: 24930734]

Paredes R, Arriagada G, Cruzat F, Villagra A, Olate J, Zaidi K, van Wijnen A, Lian JB, Stein GS, Stein JL, and Montecino M 2004 Bone-specific transcription factor Runx2 interacts with the 1alpha,25-dihydroxyvitamin D3 receptor to up-regulate rat osteocalcin gene expression in osteoblastic cells. Molecular and cellular biology. 24:8847–8861. [PubMed: 15456860]

Rojas A, Aguilar R, Henriquez B, Lian JB, Stein JL, Stein GS, van Wijnen AJ, van Zundert B, Allende ML, and Montecino M 2015 Epigenetic Control of the Bone-master Runx2 Gene During Osteoblast-lineage Commitment by the Histone Demethylase JARID1B/KDM5B. The Journal of biological chemistry.

Sepulveda H, Aguilar R, Prieto CP, Bustos F, Aedo S, Lattus J, van Zundert B, Palma V, and Montecino M 2017a Epigenetic Signatures at the RUNX2-P1 and Sp7 Gene Promoters Control Osteogenic Lineage Commitment of Umbilical Cord-Derived Mesenchymal Stem Cells. Journal of cellular physiology. 232:2519–2527. [PubMed: 27689934]

Sepulveda H, Villagra A, and Montecino M 2017b Tet-Mediated DNA Demethylation Is Required for SWI/SNF-Dependent Chromatin Remodeling and Histone-Modifying Activities That Trigger Expression of the Sp7 Osteoblast Master Gene during Mesenchymal Lineage Commitment. Mol Cell Biol. 37.

Shilatifard A 2012 The COMPASS family of histone H3K4 methylases: mechanisms of regulation in development and disease pathogenesis. Annual review of biochemistry. 81:65–95.

Sontag JM, Nunbhakdi-Craig V, Mitterhuber M, Ogris E, and Sontag E 2010 Regulation of protein phosphatase 2A methylation by LCMT1 and PME-1 plays a critical role in differentiation of neuroblastoma cells. Journal of neurochemistry. 115:1455–1465. [PubMed: 21044074]

Soutoglou E, and Talianidis I 2002 Coordination of PIC assembly and chromatin remodeling during differentiation-induced gene activation. Science. 295:1901–1904. [PubMed: 11884757]

Stein GS, Lian JB, van Wijnen AJ, Stein JL, Montecino M, Javed A, Zaidi SK, Young DW, Choi JY, and Pockwinse SM 2004 Runx2 control of organization, assembly and activity of the regulatory machinery for skeletal gene expression. Oncogene. 23:4315–4329. [PubMed: 15156188]

Tai PW, Wu H, Gordon JA, Whitfield TW, Barutcu AR, van Wijnen AJ, Lian JB, Stein GS, and Stein JL 2014 Epigenetic landscape during osteoblastogenesis defines a differentiation-dependent Runx2 promoter region. Gene. 550:1–9. [PubMed: 24881813]

Wang D, Christensen K, Chawla K, Xiao G, Krebsbach PH, and Franceschi RT 1999 Isolation and characterization of MC3T3-E1 preosteoblast subclones with distinct in vitro and in vivo differentiation/mineralization potential. J Bone Miner Res. 14:893–903. [PubMed: 10352097]

Wang P, Lin C, Smith ER, Guo H, Sanderson BW, Wu M, Gogol M, Alexander T, Seidel C, Wiedemann LM, Ge K, Krumlauf R, and Shilatifard A 2009 Global analysis of H3K4 methylation defines MLL family member targets and points to a role for MLL1-mediated H3K4 methylation in the regulation of transcriptional initiation by RNA polymerase II. Molecular and cellular biology. 29:6074–6085. [PubMed: 19703992]

Wu H, Whitfield TW, Gordon JA, Dobson JR, Tai PW, van Wijnen AJ, Stein JL, Stein GS, and Lian JB 2014 Genomic occupancy of Runx2 with global expression profiling identifies a novel dimension to control of osteoblastogenesis. Genome biology. 15:R52. [PubMed: 24655370]

Author Manuscript

Author Manuscript

Author Manuscript

Author Manuscript

Xiao ZS, Liu SG, Hinson TK, and Quarles LD 2001 Characterization of the upstream mouse Cbfa1/Runx2 promoter. Journal of cellular biochemistry. 82:647–659. [PubMed: 11500942]

Yang D, Okamura H, Nakashima Y, and Haneji T 2013 Histone demethylase Jmjd3 regulates osteoblast differentiation via transcription factors Runx2 and osterix. The Journal of biological chemistry. 288:33530–33541. [PubMed: 24106268]

Yang JW, Jeong BC, Park J, and Koh JT 2017 PHF20 positively regulates osteoblast differentiation via increasing the expression and activation of Runx2 with enrichment of H3K4me3. Scientific reports. 7:8060. [PubMed: 28808306]

Zeng PY, Vakoc CR, Chen ZC, Blobel GA, and Berger SL 2006 In vivo dual cross-linking for identification of indirect DNA-associated proteins by chromatin immunoprecipitation. BioTechniques. 41:694, 696, 698. [PubMed: 17191611]

Zhang F, Xu L, Xu L, Xu Q, Karsenty G, and Chen CD 2015 Histone demethylase JMJD3 is required for osteoblast differentiation in mice. Scientific reports. 5:13418. [PubMed: 26302868]

Zhu ED, Demay MB, and Gori F 2008 Wdr5 is essential for osteoblast differentiation. The Journal of biological chemistry. 283:7361–7367. [PubMed: 18201971]
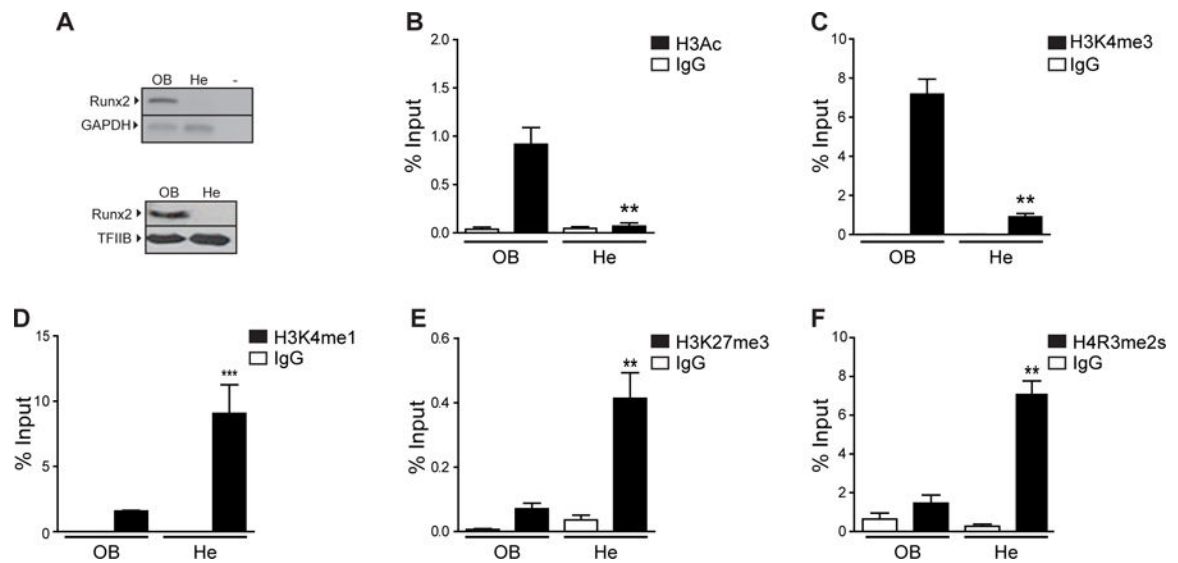
Figure 1. Histone modifications at the Runx2 P1 promoter in osteoblastic and non-osteoblastic cells.

(A) Runx2/p57 expression at mRNA (up) and protein (down) levels was analyzed by RT-PCR and western blot, respectively in samples obtained from osteosarcoma (ROS17/2.8; OB) or hepatoma (H-4-II-E; He) rat cells. Gapdh mRNA is shown as mRNA expression control. Detection of TFIIB was used to control for equal protein loading. (B-F) Enrichment of histone modifications at the Runx2 P1 promoter in osteosarcoma or hepatoma rat cells. Chromatin immunoprecipitation (ChIP) assays were performed using specific antibodies against the histone modifications (B) H3Ac, (C) H3K4me3, (D) H3K4me1, (E) H3K27me3 and (F) H4R3me2s. ChIP values are expressed as % Input ± SEM. Normal IgG was used as specificity control. Statistical analyses were performed respect to ChIP-values obtained from ROS17/2.8 cells. ***$p < 0.001$, **$p < 0.01$.
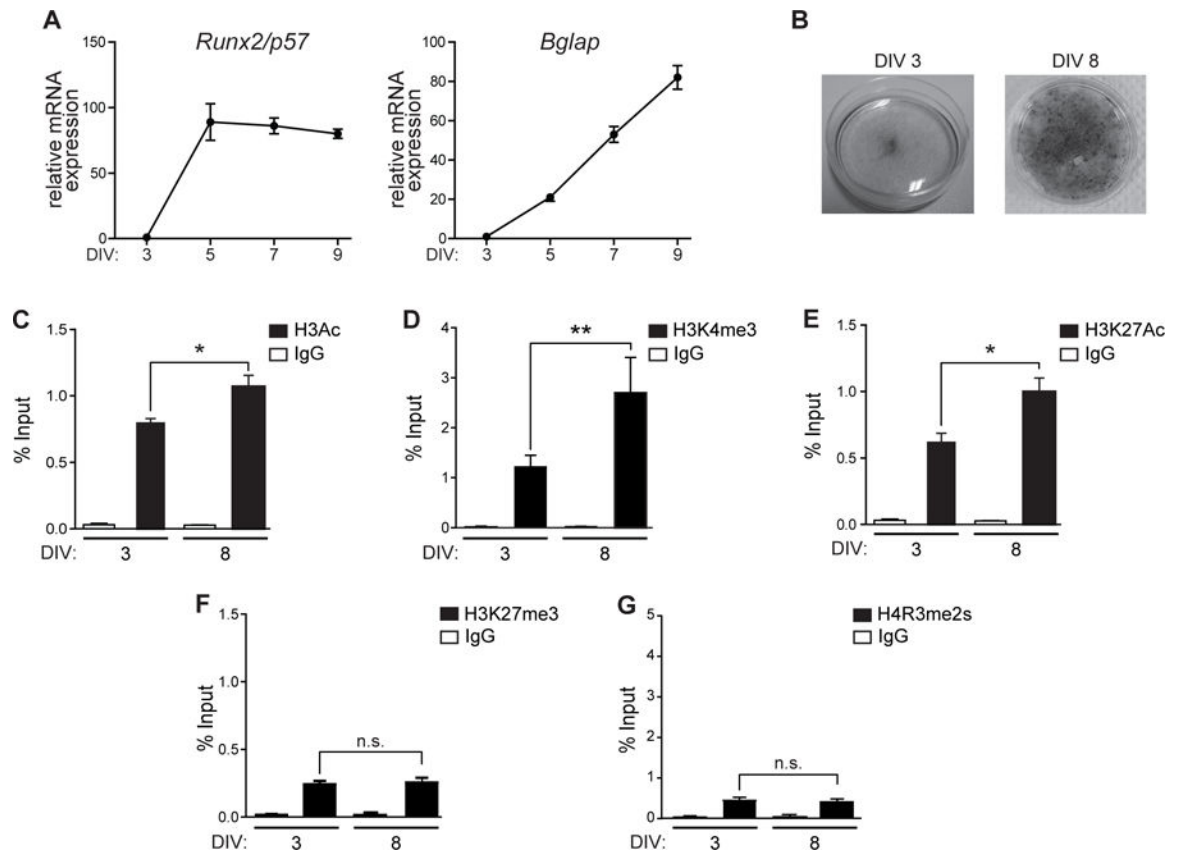
Figure 2. Epigenetic marks associated with the Runx2 P1 promoter in MC3T3 cells differentiating to osteoblasts.

(A) Runx2/p57 (left) and Bglap (right) mRNA levels are significantly upregulated during osteoblastic differentiation. MC3T3 cells treated with Ascorbic Acid (AA) 50ug/mL were collected at the indicated days and mRNA levels analyzed by RT-qPCR. mRNA expression values were normalized against Gapdh mRNA levels. (B) Alkaline phosphatase staining to determine osteoblast extracellular matrix maturation. (C-G) ChIP assays using antibodies against (C) H3Ac, (D) H3K4me3, (E) H3K27Ac, (F) H3K27me3 and (G) H4R3me2s performed at the indicated days of differentiation. Results are expressed as % Input ± SEM. Normal IgG was used as specificity control. Statistical analyses were performed with respect to 3 DIV. ***$p<0.001$, **$p<0.01$, ns = non-statistically significant differences.
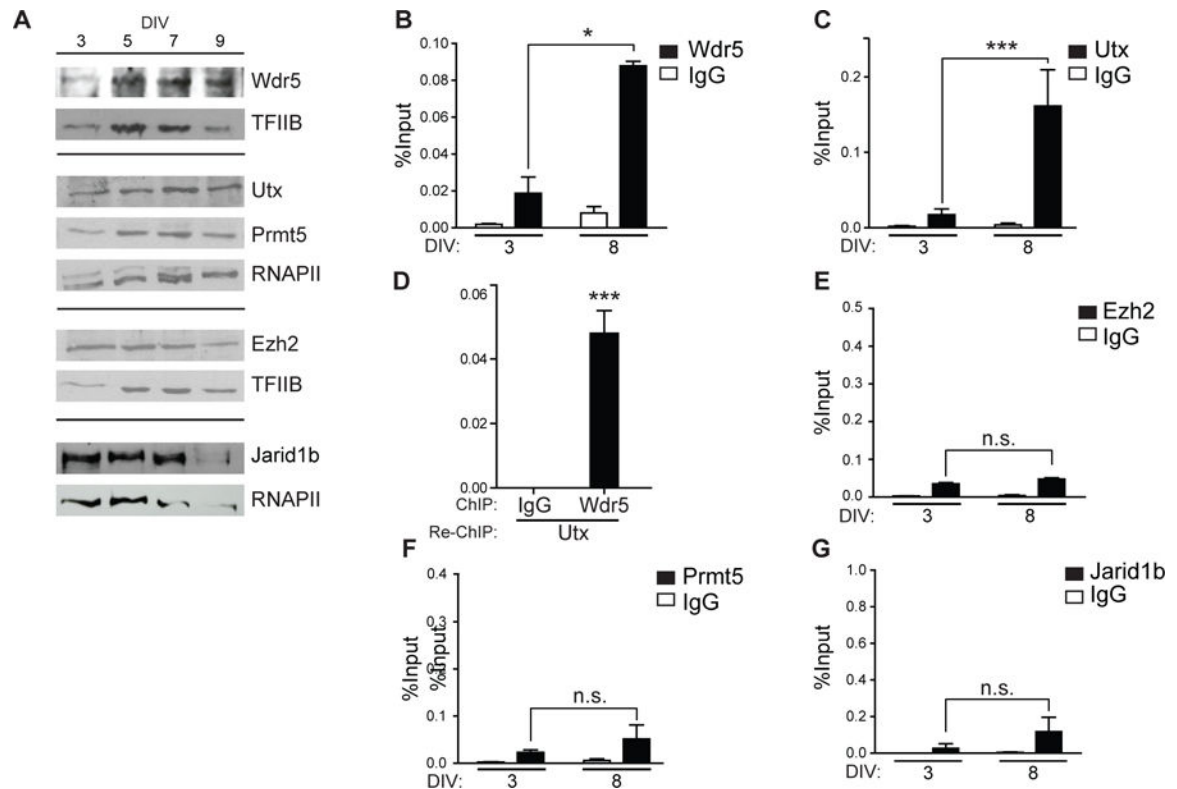
**Figure 3. Key epigenetic regulators are enriched at the Runx2 P1 promoter during osteoblast differentiation.**

(A) MC3T3 cells were differentiated to mineralized osteoblasts for 9 days of culture (DIV) using Ascorbic Acid (AA) 50ug/mL. Nuclear extracts were collected at indicated the days and analyzed by western blot using specific antibodies against the indicated epigenetic regulators. TFIIB or RNA-polymerase II (RNAPII) was used to control for equal protein loading. (B-C and E-F) Binding of chromatin regulators to the Runx2 P1 promoter at the indicated differentiation days were analyzed by ChIP using antibodies against: (B) Wdr5, (C) Utx, (E) Ezh2, (F) Prmt5, and (G) Jarid1b. (D) Re-ChIP assay performed in chromatin samples obtained from differentiated cells (5 DIV) using first an antibody against Utx and subsequently an antibody against Wdr5. Results and statistical analyses are shown as described in figure legend 2. ***p<0.001, *p<0.05, ns = non-statistically significant differences.
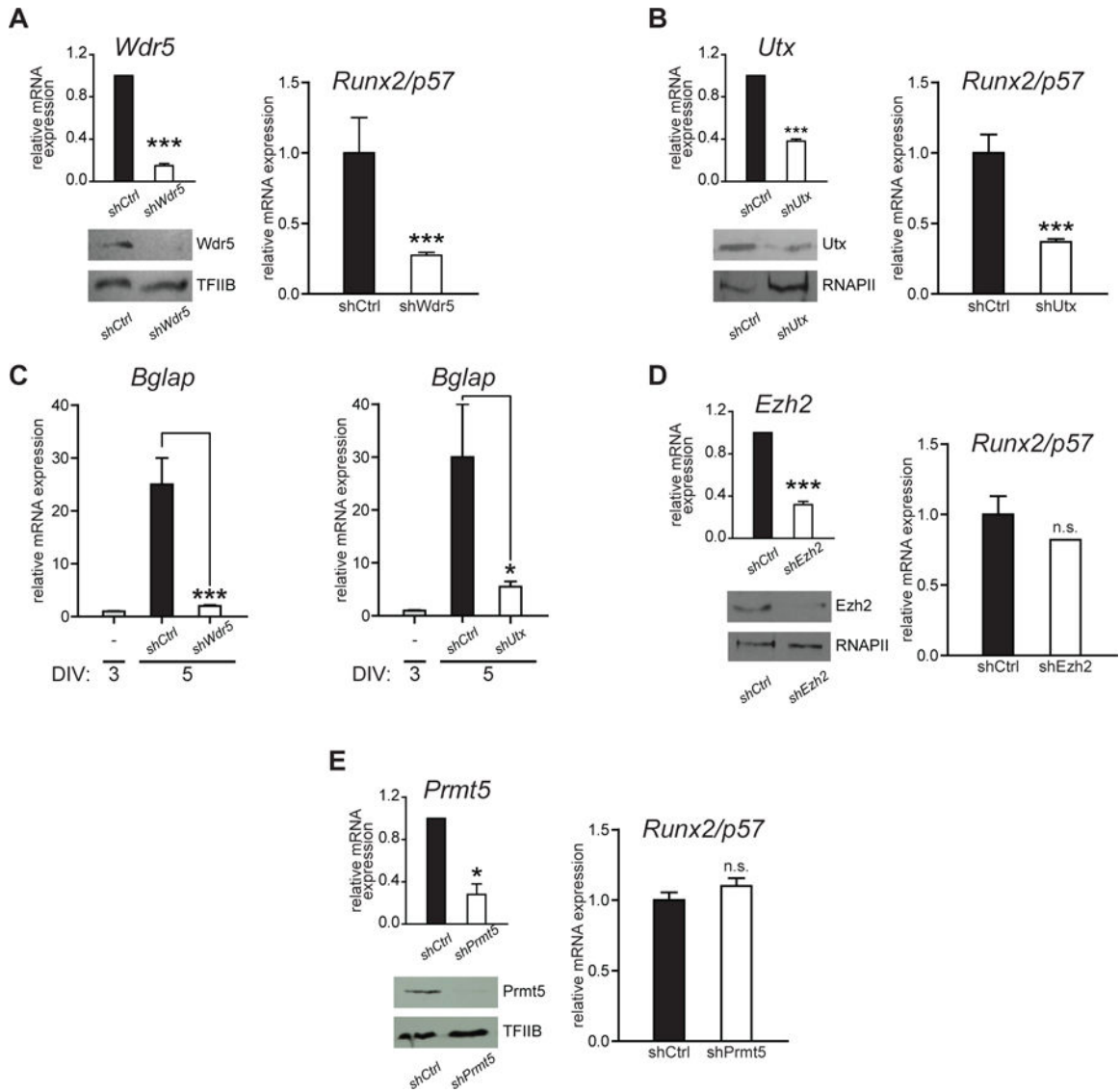
Figure 4. Knockdown of Wdr5 and Utx expression inhibits Runx2/p57 transcription in differentiating osteoblasts.

(A-B and D-E) Differentiating MC3T3 cells (3DIV) were infected with lentiviral particles containing shRNAs against the chromatin modifiers: (A) Wdr5, (B) Utx, (D) Ezh2 and (E) Prmt5. Knockdown efficiencies were confirmed by RT-qPCR and western blot (A-D, left panels) analyses, 48 h post-infection (5 DIV). TFIIB or RNAPII proteins were used to control for equal protein loading. (C) Effect of knocking down Wdr5 (left) and Utx (right) expression on Bglap gene transcription. mRNA expression values were normalized against Gapdh mRNA levels. Statistical analyses were assessed with respect to the mRNA levels obtained in cells infected with an empty vector (EV). *p<0.05, ***p<0.001, ns = non-statistically significant differences.
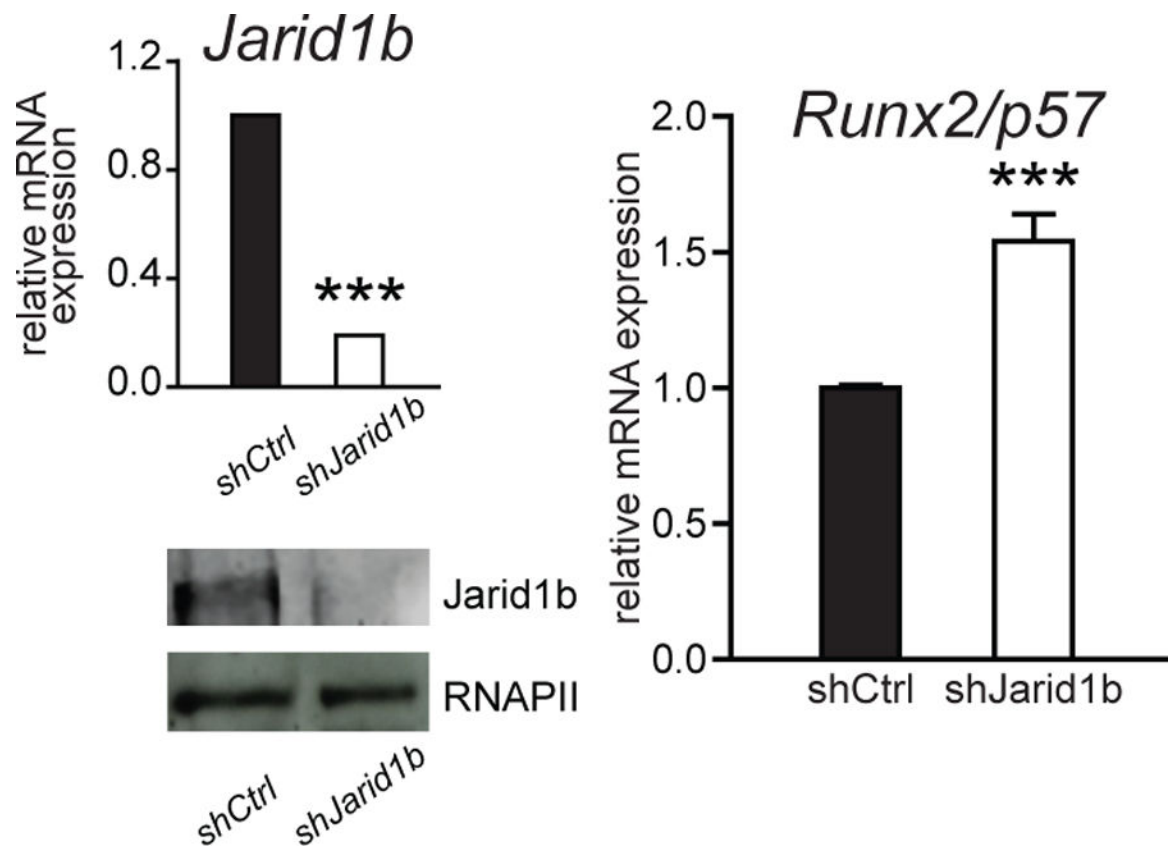
Figure 5. Runx2/p57 transcription is independent of Jarid1b function at the P1 promoter in differentiating osteoblasts.

MC3T3 (3DIV) cells were infected with lentiviral particles containing shRNAs against Jarid1b. Knockdown efficiency was determined 48 h later by RT-qPCR and western blot. RNA-Polymerase II protein was determined to control for equal loading. Runx2/p57 mRNA levels were measured by RT-qPCR normalizing against Gapdh. Statistical analyses were performed respect to mRNA levels observed in infected cells with an empty vector (E.V). ***p<0.001.
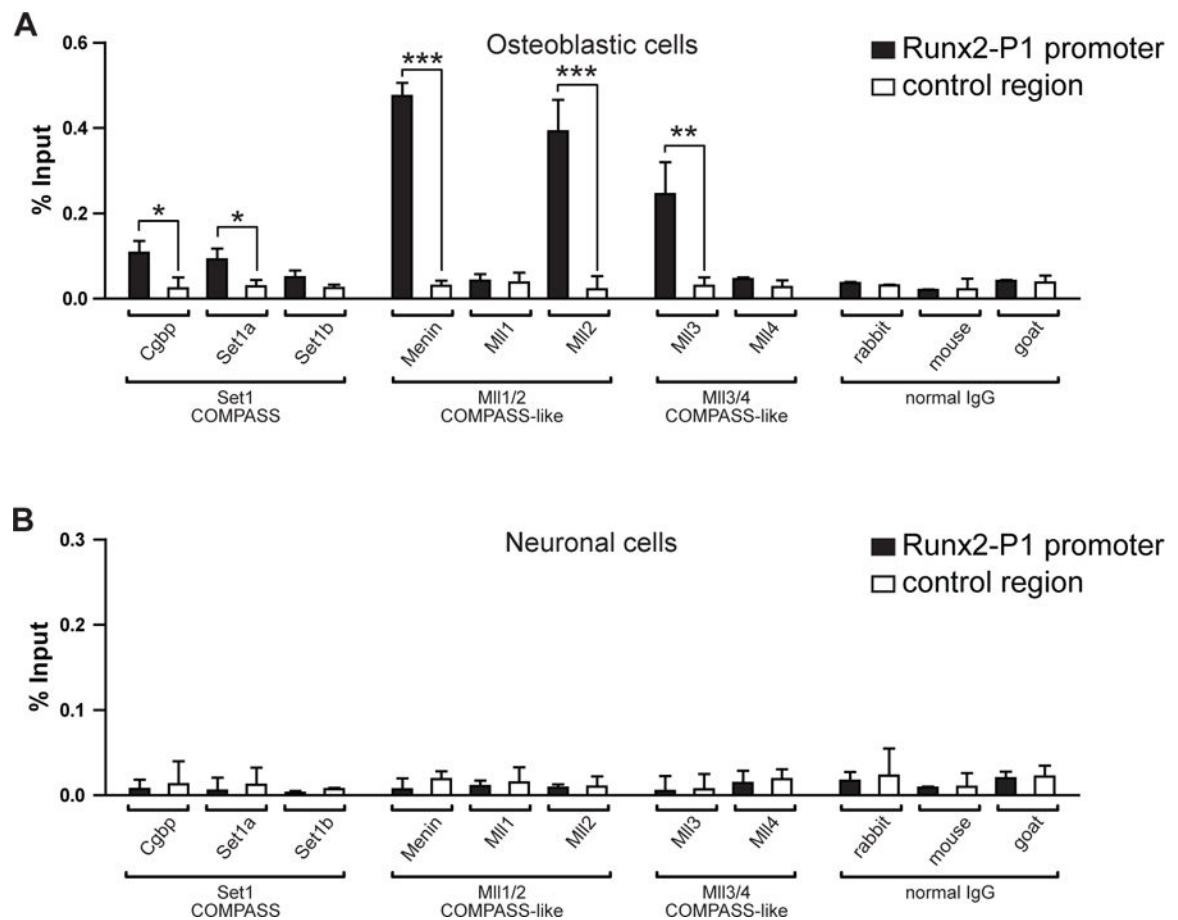
Figure 6. Mll2- and Mll3-COMPASS-like complexes are bound to the Runx2 P1 promoter in osteoblastic cells.
Differentiated MC3T3 osteoblasts (A) and N2A neuronal cells (B) were analyzed by ChIP to determine the enrichment of Cgbp, Set1a, Set1b, Menin, Mll1, Mll2, Mll3, and Mll4 proteins at the Runx2 P1 promoter region (Runx2-P1, black) and at un upstream distal region (−5Kb) of Ric8b gene promoter (control region, white). The corresponding normal IgGs were used as specificity control during each chromatin precipitation experiment. Results are expressed as % Input ± SEM. For each immunoprecipitated sample the statistical analyses were performed with respect to the control region (*p<0.05, **p<0.01, ***p<0.001). Only significant differences are indicated in graphs.